SUPPLEMENTARY INFORMATION

TITLE:

Surviving in the mountains: Temperature and elevation have contrasting physiological effects on the hoverfly *Eristalis tenax* in the Himalayas

AUTHORS:

Gauri Gharpure[1*], Jagath Vedamurthy[1,2], Sakshi Priya[3], Sunil Prabhakar[1], Geetha G Thimmegowda[1], Shannon B. Olsson[1,4*]

[1]National Centre for Biological Sciences, Tata Institute of Fundamental Research, Bengaluru, 560065, Karnataka, India

[2]Science Gallery Bengaluru, Bengaluru, 560024, Karnataka, India

[3]Independent Researcher, India

[4]the echo network, Danish Academy of Technical Sciences, 1220, Copenhagen, Denmark

* Corresponding author name(s): Gauri Gharpure, Shannon B. Olsson

Email: gauri@nicelab.science, shannon@nicelab.science

ORCID ID:

Gauri Gharpure: 0009-0006-9541-0054

Jagath Vedamurthy: 0009-0003-4358-2055

Sakshi Priya: 0009-0001-1985-2073

Sunil Prabhakar: 0000-0002-3810-7976

Geetha G Thimmegowda: 0000-0002-8523-9410

Shannon B. Olsson: 0000-0003-4126-7353

ABSTRACT:

Insect populations are experiencing a global decline due to a variety of human-linked environmental changes. Among these changes, how insects' physiology might be affected by predicted upslope migration due to climate change is unknown. Being ectotherms, insect physiology is impacted by abiotic factors like ambient temperature that change with elevation. Here, we performed in situ experiments to assess the sensory and cardiac physiology of an important generalist pollinating hoverfly Eristalis tenax (Diptera: Syrphidae), across different elevations in the eco-sensitive and biodiverse Himalayan mountains. We built a portable physiology setup and measured hoverfly antennal responses towards common floral volatiles at 3600 masl and 4200 masl. We also recorded their heart rate at 3000 masl, 3500 masl and 4000 masl. We also performed morphometric measurements on wild-caught E. tenax using micro-CT. To our knowledge, we report the first in situ physiology experiments performed in the high-altitude Himalayas and the first measurements of internal structures of wild-caught hoverfly Eristalis tenax. Our results show a contrasting impact of elevation and temperature on the sensory and cardiac physiology of hoverflies, with antennal sensitivity decreasing with increasing elevation, while average heart rate increased with temperature, independent of elevation. However, elevation did not show impact on morphometric parameters like body size and flight musculature. With upslope migration and climate warming, consequent sensory mismatches and potential cardiac stress could have deleterious effects on the health of both hoverflies and the vulnerable Himalayan ecosystem.

S1. Student t-tests assessing threshold antennal sensitivities of four floral chemicals across three elevations. Mean maximum deflections of a given dose of a tested volatile were compared to the lowest dose (10^{-5}). A statistically significant value indicates that the antennal response obtained for that dose was significantly different from the lowest dose, and that dose is classified as the threshold of antennal detection for that chemical at that elevation.

S.no.	Site	Elevation (masl)	Floral chemical/ olfactory cue	Comparison (concentration pair)	No. of pairs compared	t-value	p-value	Threshold of significant detection
(i)	Bengaluru	900	2-pentylfuran	10^{-5} and 10^{-4}	52	0.8335	0.4085	10^{-3}
(ii)	Bengaluru	900	2-pentylfuran	10^{-5} and 10^{-3}	52	3.536	**<0.0001**	
(iii)	Bengaluru	900	2-pentylfuran	10^{-5} and 10^{-2}	52	6.765	**<0.0001**	
(iv)	Bengaluru	900	2-pentylfuran	10^{-5} and 10^{-1}	52	10.72	**<0.0001**	
(v)	Kaza	3600	2-pentylfuran	10^{-5} and 10^{-4}	16	0.7645	0.4564	none
(vi)	Kaza	3600	2-pentylfuran	10^{-5} and 10^{-3}	16	0.7222	0.4813	
(vii)	Kaza	3600	2-pentylfuran	10^{-5} and 10^{-2}	16	1.527	0.1476	
(viii)	Kaza	3600	2-pentylfuran	10^{-5} and 10^{-1}	16	1.837	0.0862	
(ix)	Kibber	4200	2-pentylfuran	10^{-5} and 10^{-4}	19	0.8696	0.3959	10^{-2}
(x)	Kibber	4200	2-pentylfuran	10^{-5} and 10^{-3}	19	0.2476	0.8072	
(xi)	Kibber	4200	2-pentylfuran	10^{-5} and 10^{-2}	19	2.39	**0.028**	
(xii)	Kibber	4200	2-pentylfuran	10^{-5} and 10^{-1}	19	2.573	**0.0192**	
(xiii)	Bengaluru	900	alpha-pinene	10^{-5} and 10^{-4}	52	1.243	0.2197	10^{-2}
(xiv)	Bengaluru	900	alpha-pinene	10^{-5} and 10^{-3}	52	0.06721	0.946	
(xv)	Bengaluru	900	alpha-pinene	10^{-5} and 10^{-2}	52	5.583	**<0.0001**	
(xvi)	Bengaluru	900	alpha-pinene	10^{-5} and 10^{-1}	52	1.969	**0.0544**	
(xvii)	Kaza	3600	alpha-pinene	10^{-5} and 10^{-4}	16	1.359	0.1943	10^{-1}
(xviii)	Kaza	3600	alpha-pinene	10^{-5} and 10^{-3}	16	0.8443	0.4118	
(xix)	Kaza	3600	alpha-pinene	10^{-5} and 10^{-2}	16	1.742	0.102	
(xx)	Kaza	3600	alpha-pinene	10^{-5} and 10^{-1}	16	3.082	**0.0076**	
(xxi)	Kibber	4200	alpha-pinene	10^{-5} and 10^{-4}	19	0.0489	0.9615	10^{-2}
(xxi)	Kibber	4200	alpha-pinene	10^{-5} and 10^{-3}	19	0.7651	0.4541	
(xxiii)	Kibber	4200	alpha-pinene	10^{-5} and 10^{-2}	19	2.626	**0.0171**	
(xxiv)	Kibber	4200	alpha-pinene	10^{-5} and 10^{-1}	19	2.394	**0.0278**	
(xxv)	Bengaluru	900	cis-3-hexenyl acetate	10^{-5} and 10^{-4}	52	0.6673	0.5076	10^{-2}

(xxvi)	Bengaluru	900	cis-3-hexenyl acetate	10^{-5} and 10^{-3}	52	1.549	0.1277	
(xxvii)	Bengaluru	900	cis-3-hexenyl acetate	10^{-5} and 10^{-2}	52	9.642	**<0.0001**	
(xxviii)	Bengaluru	900	cis-3-hexenyl acetate	10^{-5} and 10^{-1}	52	10.79	**<0.0001**	
(xxix)	Kaza	3600	cis-3-hexenyl acetate	10^{-5} and 10^{-4}	16	1.442	0.1699	10^{-2}
(xxx)	Kaza	3600	cis-3-hexenyl acetate	10^{-5} and 10^{-3}	16	1.223	0.2402	
(xxxi)	Kaza	3600	cis-3-hexenyl acetate	10^{-5} and 10^{-2}	16	2.209	**0.0432**	
(xxxii)	Kaza	3600	cis-3-hexenyl acetate	10^{-5} and 10^{-1}	16	2.406	**0.0295**	
(xxxiii)	Kibber	4200	cis-3-hexenyl acetate	10^{-5} and 10^{-4}	19	1.024	0.3194	10^{-1}
(xxxiv)	Kibber	4200	cis-3-hexenyl acetate	10^{-5} and 10^{-3}	19	1.48	0.156	
(xxxv)	Kibber	4200	cis-3-hexenyl acetate	10^{-5} and 10^{-2}	19	2.05	0.0552	
(xxxvi)	Kibber	4200	cis-3-hexenyl acetate	10^{-5} and 10^{-1}	19	2.99	**0.0079**	
(xxxvii)	Bengaluru	900	p-cymene	10^{-5} and 10^{-4}	52	0.9122	0.3659	10^{-2}
(xxxviii)	Bengaluru	900	p-cymene	10^{-5} and 10^{-3}	52	0.8768	0.3847	
(xxxix)	Bengaluru	900	p-cymene	10^{-5} and 10^{-2}	52	5.381	**<0.0001**	
(xl)	Bengaluru	900	p-cymene	10^{-5} and 10^{-1}	52	12.81	**<0.0001**	
(xli)	Kaza	3600	p-cymene	10^{-5} and 10^{-4}	16	0.1058	0.9171	10^{-1}
(xlii)	Kaza	3600	p-cymene	10^{-5} and 10^{-3}	16	1.13	0.2761	
(xliii)	Kaza	3600	p-cymene	10^{-5} and 10^{-2}	16	1.866	0.0817	
(xliv)	Kaza	3600	p-cymene	10^{-5} and 10^{-1}	16	3.289	**0.005**	
(xlv)	Kibber	4200	p-cymene	10^{-5} and 10^{-4}	19	0.6305	0.5363	none
(xlvi)	Kibber	4200	p-cymene	10^{-5} and 10^{-3}	19	0.3144	0.7568	
(xlvii)	Kibber	4200	p-cymene	10^{-5} and 10^{-2}	19	1.433	0.169	
(xlviii)	Kibber	4200	p-cymene	10^{-5} and 10^{-1}	19	1.373	0.1868	

S2. 2-way Analysis of Variances (ANOVAs) comparing antennal sensitivities across three elevations of four chemicals in five doses. Elevation and dose of chemical were predictor variables and the normalized value of the maximum deflection was the response variable. The F-statistic, the corresponding p-value and degrees of freedom are reported, along with the pairs

showing significant differences in the group means obtained from post-hoc Tukey's Honest Significant Difference (HSD).

S. no.	Chemical	Comparison	F-value	p-value	Significant pairs (with post-hoc Tukey's HSD) in decreasing order of effect size	Degrees of freedom
1.	2-pentylfuran	Across doses	61.54	**< 2e-16**	Dose: 10^{-1} and 10^{-5}, 10^{-1} and 10^{-4}, 10^{-1} and 10^{-3}; Elevation: 900-4200 masl, 3600-4200 masl	4
		Across elevations	21.821	**9.64e-10**		2
		Dose*Elevation	9.923	**1.12e-12**		8
2.	α-pinene	Across doses	4.546	**0.00133**	Dose: 10^{-1} and 10^{-5}, 10^{-1} and 10^{-3}, 10^{-1} and 10^{-4}	4
		Across elevations	0.941	0.39114		2
		Dose*Elevation	0.663	0.72381		8
3.	cis-3-hexenyl acetate	Across doses	64.49	**< 2e-16**	Dose: 10^{-1} and 10^{-5}, 10^{-1} and 10^{-4}, 10^{-1} and 10^{-3}; Elevation: 900-4200 masl	4
		Across elevations	11.708	**1.13e-05**		2
		Dose*Elevation	6.655	**3.30e-08**		8
4.	p-cymene	Across doses	14.406	**4.97e-11**	Dose: 10^{-1} and 10^{-5}, 10^{-1} and 10^{-3}, 10^{-1} and 10^{-4}; Elevation: 900-4200 masl	4
		Across elevations	5.396	**0.00486**		2
		Dose*Elevation	2.121	**0.03284**		8

S3. Seasonal variation in the average heart rate of *E. tenax* at 3000, 3500 and 4000 masl at Lachen valley, Sikkim with respect to (a) elevation ($R^2 = 0.2526$, $p = 0.3931$) and (b) temperature ($R^2 = 0.05189$, $p = 0.2178$) in May; (c) elevation ($R^2 = 0.007092$, $p = 0.6202$) and (d) temperature ($R^2 = 0.2341$, $p = 0.0024$) in September. The same experiment was repeated at 3600 masl and 4200 masl in Spiti valley, Himachal Pradesh, showing variations in average heart

rate of *E. tenax* with respect to (e) elevation (R^2 = 0.01979, p = 0.5777) and (f) temperature (R^2 = 0.02580, p = 0.5243). The fitted line is generated by logistic regression with shaded areas showing 95% confidence intervals. The statistical differences between seasons could be because the temperatures in Sikkim have different variation (7°C in May vs. 12°C in September) and are significantly different (t = 4.8266, p < 0.0001) in May vs. September (also see Table S8(iv)). We were able to better capture the variation in the abiotic conditions in September, while we could sample limited a temperature range in Spiti valley, Himachal Pradesh.

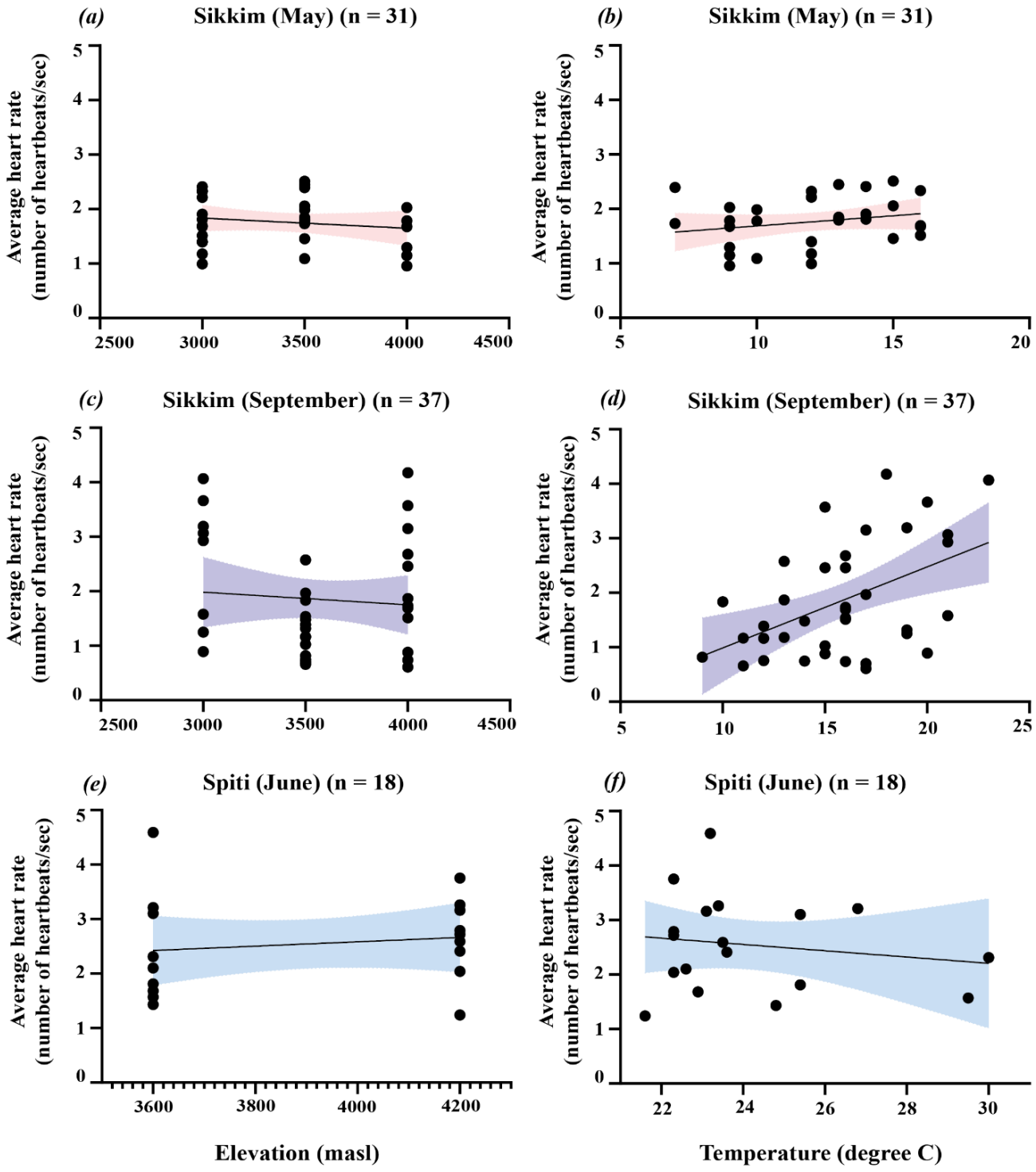

S4. Recipe for positive control olfactory blend (from Nordström et al., 2017):

Chemical	CAS number	Vapour pressure	Amount (µl)
2-ethyl toluene	611-14-3	2.1 mm Hg at 20 °C	16.1
p-cymene	99-87-6	1.50 mm Hg at 25 °C	11.8
R-limonene	5989-27-5	1.00 mmHg at 20 °C	24.1
undecanal	112-44-7	0.08 mmHg at 25 °C	50
6-methyl-5-hepten-2-one	110-93-0	1.28 mmHg at 25 °C	17.3
mineral oil	8042-47-5	negligible	82.7

S5. Normalised values of maximum deflection towards the 10^{-1} dose plotted against the variation of temperatures for each volatile, where the fitted line is generated by logistic regression with outliers included in the analyses (a) 2-pentylfuran ($R^2 = 0.01911$, $p = 0.2017$), (b) alpha-pinene ($R^2 = 0.003005$, $p = 0.614$), (c) cis-3-hexenyl acetate ($R^2 = 0.02103$, $p = 0.1801$). Ambient temperature had no significant effect on the antennal responses of the animals to any volatile.

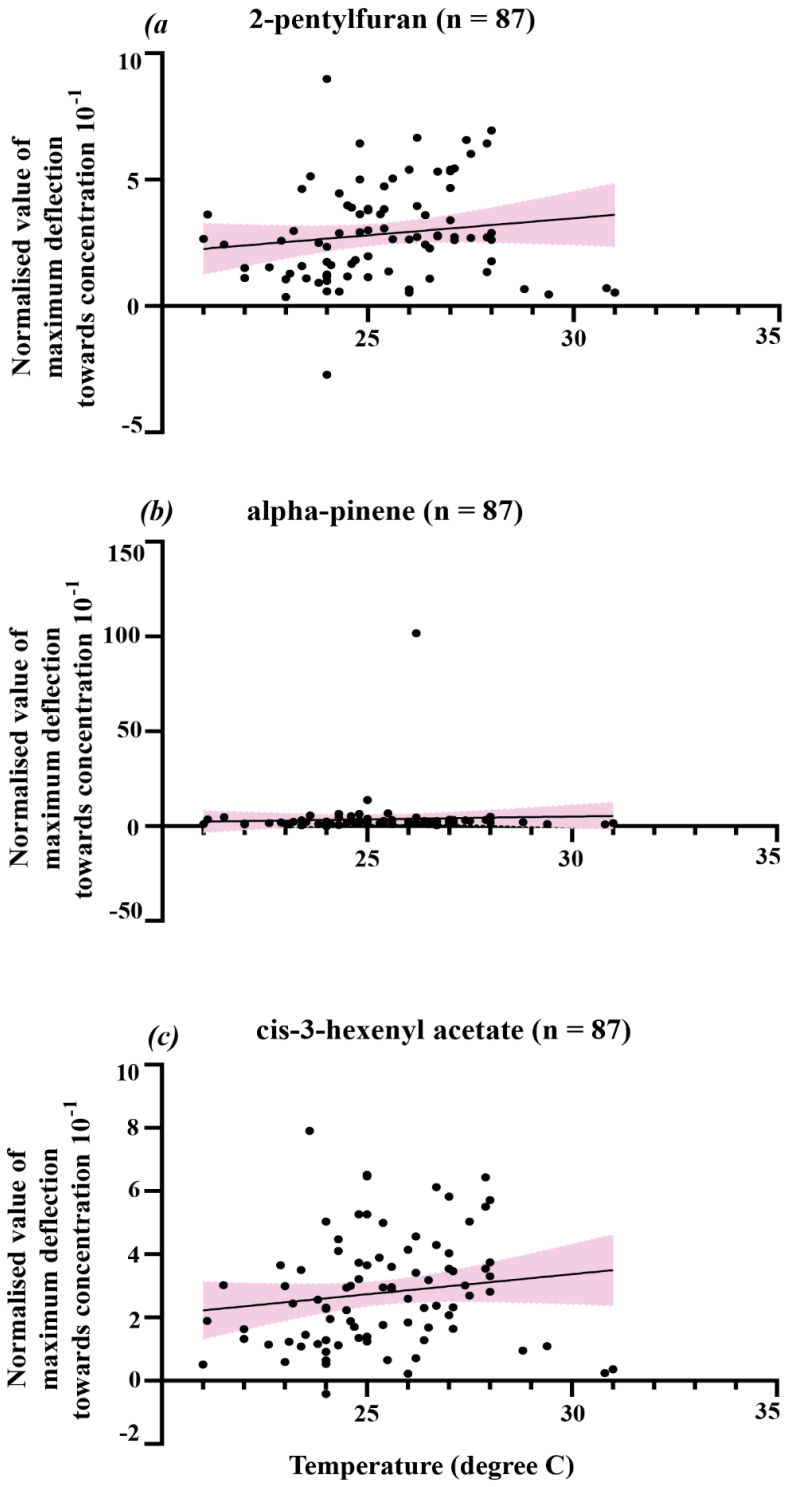

S6. Video S1: sample heartrate recording (trimmed) of *Eristalis tenax*

S7. Summary table of results of generalised linear mixed-models (GLMMs) for analyses of electroantennograms

S. no.	Response variable	Predictor variable		Estimate	p-value	Significance level	Sample size
(i)	Normalised value of deflection to all chemicals	Fixed effect 1	Elevation	1.24E-04	**1.02E-13**	***	86
		Fixed effect 2	Temperature	3.26E-03	0.7732	ns	86
		Fixed effect 3	Dilution	2.22E-01	**< 2e-16**	***	86
		Fixed effect 4	Elevation * Temperature	-7.52E-06	**< 2e-16**	***	86
		Random effect	Individual ID	NA	NA	NA	86
(ii)	Normalised value of deflection to 2-pentylfuran	Fixed effect 1	Elevation	3.81E-04	**< 2e-16**	***	86
		Fixed effect 2	Temperature	1.70E-02	0.389	ns	86
		Fixed effect 3	Dilution	2.18E-01	**< 2e-16**	***	86
		Fixed effect 4	Elevation * Temperature	-1.98E-05	**< 2e-16**	***	86

		Random effect	Individual ID	NA	NA	NA	86
(iii)	Normalised value of deflection to α-pinene	Fixed effect 1	Elevation	3.26E-04	**<2e-16**	***	86
		Fixed effect 2	Temperature	3.09E-02	0.119	ns	86
		Fixed effect 3	Dilution	1.97E-01	**<2e-16**	***	86
		Fixed effect 4	Elevation * Temperature	-1.39E-05	**<2e-16**	***	86
		Random effect	Individual ID	NA	NA	NA	86
(iv)	Normalised value of deflection to cis-3-hexenyl acetate	Fixed effect 1	Elevation	5.87E-05	**0.0378**	*	86
		Fixed effect 2	Temperature	7.20E-03	0.7027	ns	86
		Fixed effect 3	Dilution	2.45E-01	**<2e-16**	***	86
		Fixed effect 4	Elevation * Temperature	-4.40E-06	**<2e-16**	***	86
		Random effect	Individual ID	NA	NA	NA	86

(v)	Normalised value of deflection to p-cymene	Fixed effect 1	Elevation	-4.04E-04	**< 2e-16**	***	86
		Fixed effect 2	Temperature	-5.67E-02	**0.000588**	***	86
		Fixed effect 3	Dilution	1.88E-01	**< 2e-16**	***	86
		Fixed effect 4	Elevation * Temperature	1.33E-05	**< 2e-16**	***	86
		Random effect	Individual ID	NA	NA	NA	86

S8. Summary table of results of generalised linear mixed-models (GLMMs) for analyses of average heart rate

S. no.	**Response variable**	**Predictor variable**		**Estimate**	**p-value**	**Significance level**	**Sample size**
(i)	Average heart rate in all sites	Fixed effect 1	Elevation	2.17E-04	**2.90E-03**	**	137
		Fixed effect 2	Temperature	7.11E-02	**2.19E-05**	***	137
		Random effect	Individual ID	NA	NA	NA	137
(ii)	Average heart rate	Fixed effect 1	Elevation	6.46E-05	0.795267	ns	68

	in Sikkim (3000, 3500, 4000 masl)	Fixed effect 2	Temperature	8.80E-02	**0.000926**	***	68
		Random effect	Individual ID	NA	NA	NA	68
(iii)	Average heart rate in Bengaluru (900 masl)	Fixed effect 1	Temperature	4.04E-01	**0.0415**	*	51
		Random effect	Individual ID	NA	NA	NA	51
(iv)	Average heart rate in Spiti (3600, 4200 masl)	Fixed effect 1	Elevation	1.92E-04	0.819	ns	18
		Fixed effect 2	Temperature	-4.29E-02	0.686	ns	18
		Random effect	Individual ID	NA	NA	NA	18

S9. The transverse section of *Eristalis tenax* thorax. The dosro-longitudinal muscles (DLMs) and dosro-ventral muscles (DVMs) are visible in the centre of the thoracic cavity. The numbers mark distinct dorso-longitudinal muscle bundles.

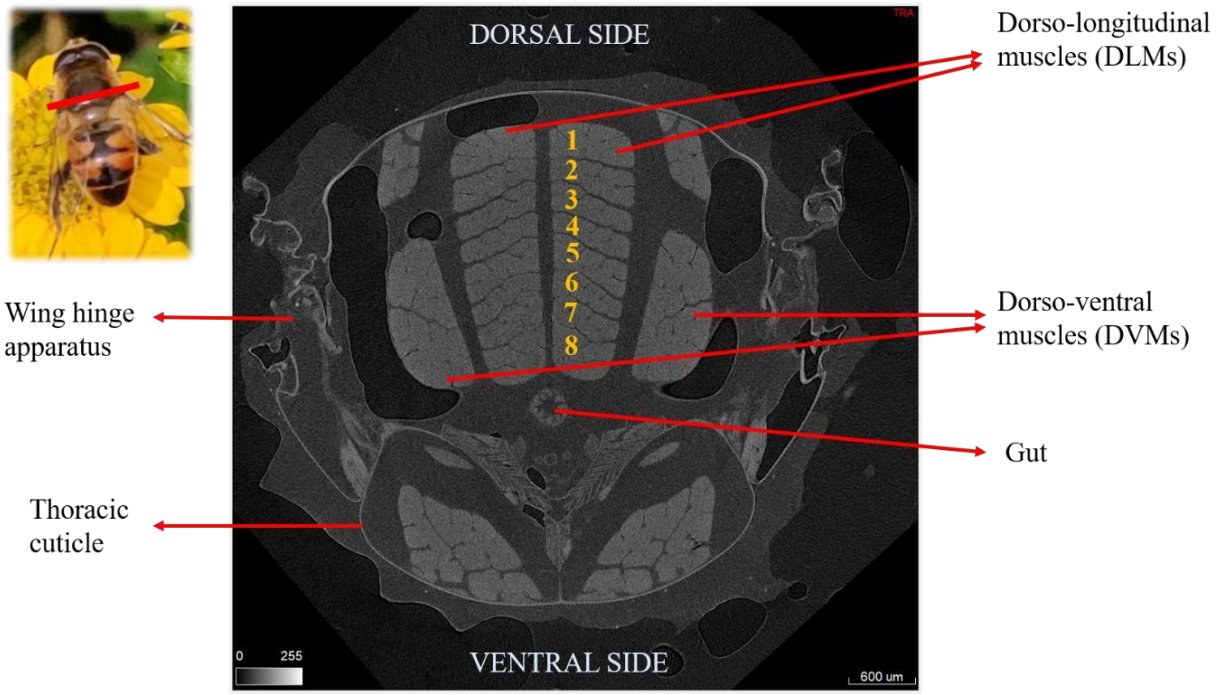

We marked Regions of Interest (ROIs) using CTAnalyser (CTAn; Bruker Instruments) in the tissues and regions of interest. The following ROIs were drawn: (1) whole body (this was done on the 8x downsized version of the whole animal for ease of data handling, and then mapped onto the 4x downsized version for further calculations), (2) dorsolateral muscles (DLMs) and (3) dorso-ventral muscles (DVMs). The whole body and DLM ROIs were drawn on the transverse views, while the DVMs were drawn on the coronal view. Hence, the DVMs were 3D-registered onto the whole body in the transverse view and then used for further assessments.

The software CTan was then employed to perform operations on these ROIs as follows:

(1) Whole body ROI: This ROI was first drawn onto the 8x downsized version to enable us to handle the large dataset in the limited computer RAM. The ROI was drawn as close to the body outline as possible to remove artefacts like legs. CTAN was then used to generate the body outline by identifying the outline inside the ROIs. In the slices where there were breaks in the outline (due to improper staining, or break in the cuticle itself at wing hinges etc.), the ROIs drawn above were

used as a proxy of body outline since they were drawn very close to the actual outline of the body. Thus, a closed outline of the entire body was generated an and void spaces within the outline were deleted for further calculations.

(2) DLM ROI: The ROIs for DLMs were drawn around the entire DLM. The image of the muscle bundles inside the ROI was then extracted using the threshold function, and then converted into a bitmap image. The resulting black and white image stack in bitmap format was then used to perform further volume calculations.

(3) DVM ROI: The DVMs were better visualized in the coronal view, hence the coronal view of the thorax was first saved separately. The ROI for each DVM bundle was drawn separately, resulting in 6 DVM drawing for each animal (3 each on left and right of the thorax). The 6 ROIs were then stitched together to form one bitmap image with 6 DVM ROIs. These ROIs were then registered onto the whole body in the transverse view using the 3D registration function in DataViewer software (Bruker Instruments, Version 1.7.0.1). This allowed further calculations for the animal to be conducted together in the transverse view. The DVM ROIs were further converted into black and white images using the same method as used for the DLMs.

Once all the ROIs were converted into the bitmap format, they were again imported into CTAn. The images were first subjected to filtering, closing of margins and pores and despeckling to yield complete ROIs which encompass our tissue of interest.

S10. Summary table of results of linear regression models for analyses of variation of body size parameters

S. no.	Predictor variable	Response variable	Estimate	Standard error	p-value	Sample size

(i)	Elevation	Body length	7.621e-04	1.144e-03	0.51427	19
(ii)	Elevation	Thorax volume	0.005612	0.005509	0.3227	19
(iii)	Elevation	Body volume	0.01263	0.01373	0.3706	19
(iv)	Elevation	DLM+DVM volume/thorax volume	1.319e-05	2.999e-05	0.666	19
(v)	Elevation	DLM+DVM volume/body volume	6.156e-06	1.303e-05	0.643	19
(vi)	Elevation	DLM volume/thorax volume	9.387e-06	1.702e-05	0.588	19
(vii)	Elevation	DLM volume/body volume	4.352e-06	7.476e-06	0.568	19
(viii)	Elevation	DVM volume/thorax volume	3.798e-06	1.351e-05	0.7820	19
(ix)	Elevation	DVM volume/body volume	1.804e-06	5.794e-06	0.7594	19
(x)	Elevation	DLM surface area	0.03773	0.03142	0.246	19

(xi)	Elevation	DVM surface area	-0.001759	0.027756	0.950	19
(xii)	Thorax volume	DLM volume	0.17546	0.05132	**0.00327**	19
(xiii)	Body volume	DLM volume	9.014	2.062	**0.000328**	19
(xiv)	Thorax volume	DVM volume	0.16644	0.03619	**0.000256**	19
(xv)	Body volume	DVM volume	12.192	2.237	**2.93e-05**	19
(xvi)	Thorax volume	DLM surface area	4.1541	0.9699	**0.000503**	19
(xvii)	Body volume	DLM surface area	1.7720	0.3652	**0.00015**	19
(xviii)	Thorax volume	DVM surface area	3.3111	0.8732	**0.00146**	19
(xix)	Body volume	DVM surface area	1.3995	0.3372	**0.00067**	19
(xx)	Thorax volume	DLM+DVM surface area	7.465	1.529	**0.00014**	19
(xxi)	Body volume	DLM+DVM surface area	3.1715	0.5672	**3.24e-05**	19